C.C. NEACSU
G.A. STEUDLE
M.B. RASCHKE✉

Plasmonic light scattering from nanoscopic metal tips

Max-Born-Institut für Nichtlineare Optik und Kurzzeitspektroskopie, 12489 Berlin, Germany

ABSTRACT Linear light scattering by individual nanoscopic metal wire tips is investigated. Using evanescent-wave excitation, the spectral and polarization dependence of the emission are addressed. Choosing gold and tungsten as representative tip materials, intense scattering and a strongly plasmon-resonant behavior observed for gold contrasts a comparatively weak and spectrally flat response for tungsten. Spectral dependence and local-field enhancement are found to be sensitive to details of the structural parameters and can be described by a simple model. The results provide selection criteria for tips to be used in scattering-type near-field microscopy or for photoemission in inelastic tunneling spectroscopy.

PACS

1   Introduction

Antennas are structures designed for radiating or receiving electromagnetic waves and concomitant energy transfer to or from a confined volume [1]. Currently, much effort is devoted to scaling dimensions down to the optical regime. Related interests range from an understanding of the fundamental differences compared to the radio-frequency range [2, 3] to the design and manufacturing of sophisticated device structures for guiding and switching light, optical computing, and chemical and biological sensor applications [4, 5].

One of the simplest and most widely used structures in this respect which stands out in particular for its simplicity is the tapered tip used as a sensor in scanning probe microscopy. Whereas the optical characteristics of dielectric tips have intensely been investigated because of their importance as probes for scanning near-field microscopy (SNOM) [6], in contrast, the optical properties of metallic tips have received comparatively little attention. Despite their widespread application as probes in scanning-tunneling microscopy (STM) and atomic-force microscopy, it has only recently been proven fruitful to take advantage of their optical properties as well. This allows for ultra-high spatial resolution down to several nanometers in combination with the unique material and chemical specificity provided by the optical response.

✉ Fax: +49-30-63921489, E-mail: raschke@mbi-berlin.de

This has successfully been demonstrated in particular in photoemission by inelastic tunneling in scanning-tunneling microscopy [7] and scattering-type scanning near-field optical microscopy (s-SNOM) [8–11] providing optical spectroscopy on the nanoscale.

With both techniques relying on light scattering from, in general, metallic probe tips their performance depends critically on the degree of confinement of the optical field at the tip apex. Much experimental and theoretical effort (see e.g. [2, 9, 12–14] and references therein) has therefore been devoted to the understanding of the local-field enhancement at sharp tips or related model structures. However, the spectral characteristics of the optical response of the tip is of profound importance as well. When probing electronic and dielectric properties of a medium by means of the aforementioned techniques, the spectral response of the probe tip has to be known [16, 31]. In addition, for certain metals, the excitation of localized surface plasmons at the tip apex would allow for resonant enhancement of the local field at the driving laser frequency and thus for greater sensitivity and contrast. Also, with the tip structure being frequently invoked as a model system to explain surface enhancement of, for example, Raman scattering from rough metal surfaces [17, 18], a detailed knowledge of its optical response is desirable.

In this work, the spectral and polarization characteristics of light scattering from individual sharp metal tips is investigated. Whereas for tungsten as tip material the optical response is found to be only weakly wavelength selective, in contrast, for gold the scattering process is characterized by a plasmon-resonant behavior. The details of the spectral response are seen to depend sensitively on morphology and size of the tips as well as surrounding medium and field polarization. A simple electrostatic model can be applied to consistently describe the rich behavior observed and the results are discussed within the framework of antenna theory.

2   Experiment

In our experiment we use dark-field scattering spectroscopy based on evanescent-wave excitation at a dielectric interface. Here, a parallel white-light beam from a halogen-bulb lamp is directed on to the base of a quartz prism under total internal reflection conditions as depicted in Fig. 1a. The scattered light from the tip when penetrating into the evanescent-field region is collected in the direction
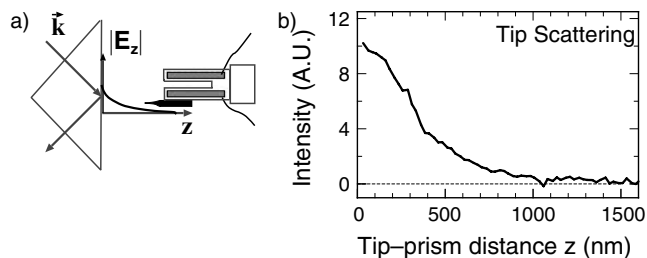
FIGURE 1   Schematics of the experimental setup (**a**). The spectral characteristics of the light scattered by the metal tip frustrating the evanescent light field produced by total internal reflection are measured. The corresponding distance dependence of the spectrally integrated response is shown for a tip approaching the prism surface (**b**)

perpendicular to the incidence plane by means of a long working distance microscope objective (working distance = 20.5 mm, numerical aperture (NA) = 0.35) and detected using an imaging spectrograph with a liquid nitrogen cooled charged coupled device (CCD). The tips are attached to a quartz tuning fork of a shear-force-based atomic-force microscope (AFM) and spectra are recorded with the tip within several nanometers proximity to the prism surface.

The evanescent field formed at the quartz interface is given by

$$E_t(z, \omega) \propto E_0(\omega) e^{-k(\omega)z\sqrt{\sin^2\alpha - n(\omega)^2}},$$

with wavevector $k(\omega)$ in the optically dense medium and the frequency-dependent index of refraction $n(\omega)$ [19]. With the metal tip frustrating the evanescent field as it penetrates into the near-field region this gives rise to the characteristic tip–prism distance dependence of the spectrally integrated scattering signal as shown in Fig. 1b. The excitation is thus limited to the near-apex region within several 100 nm from the tip end. This leads to a greatly reduced background compared to, for example, dark-field scattering based on far-field illumination.

Radially symmetric Au and W tips were obtained by electrochemical etching [20]. For tungsten tips a W wire (Ø = 200 μm) is immersed by about 2–3 mm into 2 M KOH, centered inside a stainless steel cylindrical cathode and biased by +3.0 V. For the gold tips a 1:1 mixture of HCl (aq. 37%) and ethanol serves as electrolyte and a Pt wire ring (Ø ∼ 1 cm) cathode positioned at the liquid surface is used (tip bias +2.2 V). Before etching, the cleaned Au and W wires are carefully aligned perpendicular to the electrolyte surface. The DC etch voltage is provided by a source with a fast cut-off circuit which breaks the voltage when the immersed portion of the wire falls off [20]. This, together with fresh electrolyte, a homogeneous meniscus, low vibration, and an air-draft-free environment during etching ensures regular tip shapes and smooth shaft surfaces. After etching the tips are cleaned in purified water and stored in isopropanol prior to use. For the tips obtained, apex radii ranged from ≲ 10 to 50 nm as characterized by electron microscopy.

3   Results

Representative scattering spectra for different Au and W tips for unpolarized excitation and detection are shown in Fig. 2. The data are background corrected and normalized
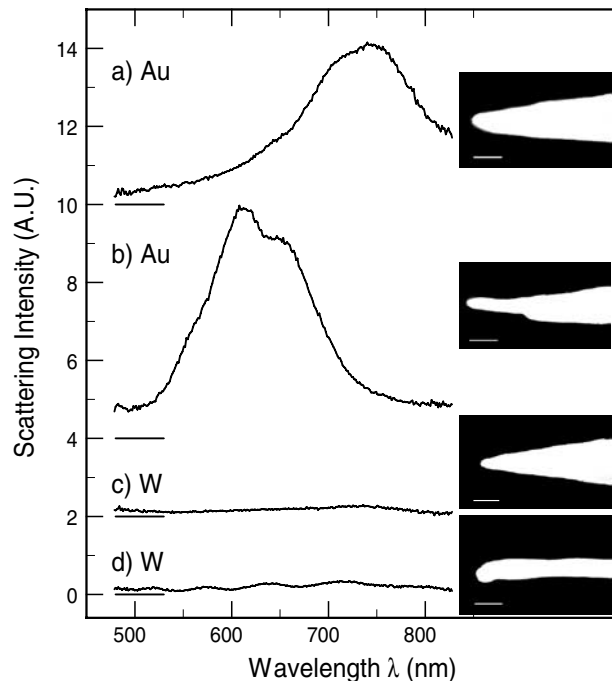
FIGURE 2   Scattering spectra for different Au and W tips. For regular Au tips the optical response is characterized by a plasmon-resonant behavior (**a**), becoming increasingly structured for irregular tip shapes (**b**). For tungsten, weaker scattering intensities and an in general spectrally flat response are observed (**c**), except for very large aspect ratios in which some spectral modulation can be observed (**d**). Electron micrographs for the tip structures investigated (*right*) are presented. The scale bar corresponds to 100 nm

with respect to the excitation-lamp spectrum and the spectral instrument response function. The spectral data are juxtaposed with the electron-microscope image from the corresponding tip. For W tips, in general, a spectrally flat optical response is observed with weak overall scattering intensities (Fig. 2c). The spectral behavior is found to show little variation with tip radius and tip cone angle. This is except for the case of very slender tips where a modulation is observed, as shown in Fig. 2d. In contrast, for the Au tips, the scattering intensity is strongly wavelength dependent, characteristic for a plasmon-resonant behavior. Also, off-resonant higher overall emission intensities are observed compared to W. Both scattering intensity and spectral position of the resonance are found to be very sensitive to structural details. While for regular tip shapes the resonance is characterized by one (Fig. 2a) (or two, as will be discussed below) distinct spectral features, inhomogeneities in the geometric shape result in irregular peaks (Fig. 2b). It should be noted, however, that in several instances despite a regular tip shape the spectral response defied the characteristic signature of a plasmon resonance. Here, throughout the accessible spectral range of 400–1100 nm the scattering intensities were found to be of the order of the typical off-resonant signal levels comparable to the data shown in Fig. 2a and b. In general, the results seem to indicate that the plasmon resonance shifts to shorter wavelengths with decreasing tip radii. However, as will be discussed in detail below, the spectral position and shape of the plasmon resonance also depend sensitively on the aspect ratio of the tip.

An interesting behavior is observed by studying the polarization dependence of the tip scattering process. Here, the
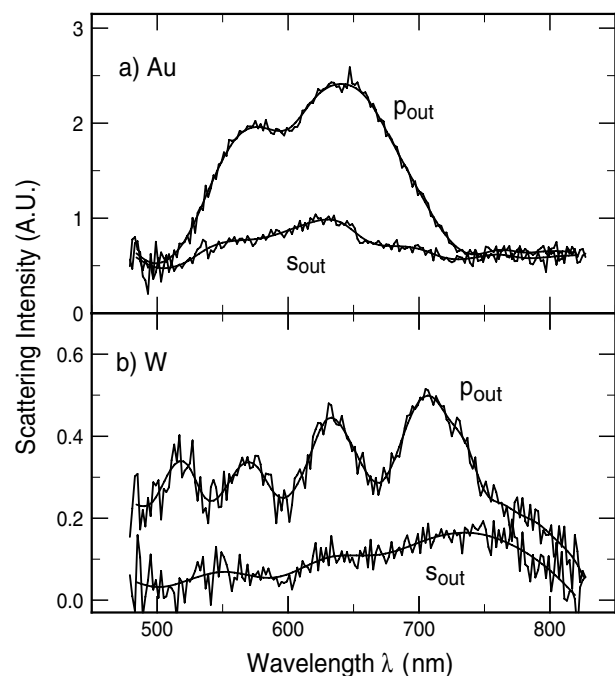
FIGURE 3 Polarization dependence of scattering spectra. **a** Au tip with slightly irregular shape gives rise to a featured plasmon resonance in *p*-polarization which nearly vanishes when emission is detected polarized perpendicular to tip axis (*s*). The near-negligible polarization contrast when probing off-resonantly has frequently been observed for Au tips. **b** Example for W tip with very large aspect ratio. Except for the spectral variation in *p*-polarized detection the behavior is typical for most W tips investigated (note: data normalized with respect to the difference in pump field intensities for the evanescent electric field components oriented ⊥ and ∥ to the prism surface)

FIGURE 4 Resonant light scattering from an Au tip where the two distinct resonances (**a**) can be attributed to the excitation of the plasmon oscillations perpendicular (*s*) and parallel (*p*) with respect to the tip axis, respectively, as evident from the polarization-resolved study (**b**). The incomplete discrimination between the two plasmonic contributions can be attributed to slight deviations from the parallel alignment of the rotational axis of the tip apex region with respect to the surface normal

polarization directions are defined as parallel (*p*) and perpendicular (*s*) with respect to the plane formed by the incoming wave vector $k(\omega)$ and the surface normal n of the prism base. In general, stronger emission is observed for the electric field detected parallel to the tip axis (*p*-polarized emission) for both Au and W tips. The intensity ratio of *p* to *s* is typically found in the range between 2 and 5 with a maximum value of ∼ 10. For gold tips, the difference in scattering intensity between the two polarization states is most pronounced at the plasmon resonance with only small to near-negligible off-resonance contrast as seen in Fig. 3a. In contrast, for W the ratio of *s* to *p* emission is only weakly wavelength dependent. The data shown in Fig. 3b represent the limiting case in that respect for the W tip with the exceptionally large aspect ratio shown in Fig. 2d.

Studying the polarization dependence can provide further information on the nature of the plasmon resonance. As discussed above, the occurrence of a spectrally structured plasmon response can be the result of irregularities of the kind shown in the electron micrograph of Fig. 2b. These geometric features effectively lead to a spatial variation of the confinement of the correlated electron motion in the axial direction at the tip apex, and can thus give rise to in general different oscillation frequencies. In that case in *s*-polarized emission both resonant features would diminish simultaneously, as seen in Fig. 3. However, favorable conditions for the formation of a radiating plasmon resonance can also occur for excitation with the electric field aligned perpendicular to the tip axis. Thus, in unpolarized detection this would give rise to two distinct resonance features as shown in Fig. 4a. Depending on polarization, these different contributions from the longitudinal and transversal plasmon resonances can then be separated as shown in the lower panel. In this situation the *s*-polarized emission intensity can exceed *p*-polarized emission intensity within certain wavelength regions—in contrast to those tips which only allow for an axial plasmon excitation. However, comparing the topologies of the tips shown and other data for different tips investigated, we were not able to identify the relevant structural parameter responsible for whether a tip supports just one or both, axial and sagittal, plasmon excitations.

This behavior in particular, and the in general small polarization ratios discussed above, seem to contrast expectations based on theoretical modeling of the electric field near the tip apex region. There, from the calculated large enhancement when the electric field is oriented parallel to the tip axis compared to the perpendicular direction [2, 9], strongly enhanced scattering for *p*-polarization should result. From the experimental point of view, a possible reason for the reduced polarization contrast even for an ideal tip is the fact that the induced surface current density is very sensitive to the exact orientation of the applied electric field. Thus, for realistic structures small deviations from the rotational symmetry, surface inhomogeneities, or other structural imperfections, which are difficult to control given the preparation procedure, would give rise to a possibly complex form of the induced polarization [23, 25].

In the experimental geometry used, the excitation is limited to the outermost several 100 nm of the tip end, given by the spatial extent of the evanescent field. Yet, the characteristic spectroscopic response of the tip is solely determined by this near-apex region of the tip. This is concluded from far-field spectroscopy, which we carried out for comparison using direct illumination exciting a tip region of several µm. Here, essentially the same spectral dependence is observed, only offset in scattering intensity by a large spectrally unspecific background.

4   Model calculation and discussion

From the experiments shown and series of other spectra taken for different tips we conclude that the details of the optical response in terms of scattering intensity, and shape and spectral position of the resonance, depend sensitively on structural details of the tip apex region. Despite this rich behavior observed, the experimental results can be rationalized with a simple model. Here, as an approximation of the tip geometry we treat it as a small hemispheroid with semimajor and semiminor axes a and b, respectively. In the following we will show that this qualitatively describes the experimentally observed trends in the optical response of the tips with regard to: (a) dependence on tip material, (b) tip apex shape, (c) scattering intensity, (d) spectral characteristics, and (e) polarization characteristics.

This model has been applied earlier to describe the electromagnetic mechanism of surface enhancement of Raman scattering [18, 21] and second-harmonic generation from rough surfaces [22]. To match the boundary conditions the hemispheroid is situated with its base on an infinite plane, which, for simplicity, is taken to be a perfect conductor. In the limiting case of the relevant dimensions of the structure being small compared to the wavelength (i.e. $ka \ll 1$), it can be treated in the quasistatic response to an incident optical field, yet with the excitation-frequency dependence of the electric susceptibility of the hemispheroid taken explicitly into account. The polarizability α_i of this hemispheroidal protrusion in a uniform field parallel to one of its principal axes is then given by

$$\alpha_i(\omega) = \frac{4\pi a b^2}{3} \frac{\epsilon_t(\omega) - \epsilon_m(\omega)}{\epsilon_m(\omega) + A_i[\epsilon_t(\omega) - \epsilon_m(\omega)]}, \quad (1)$$

with ϵ_t and ϵ_m the permittivities of the tip and the surrounding medium (here, $\epsilon_m \approx 1$ for air), respectively, and A_i being the depolarization factor, a function of the structural parameters a and b only [23]. The depolarization factor A takes on the value of 1/3 for a sphere and approaches 0 for a very slender prolate spheroid.

This model has the virtue of allowing the direct visualization of the dependence of the polarizability and thus the scattering efficiency on tip material and structural parameters. The hemispheroid exhibits a resonant response to the applied field when $\text{Re}[\epsilon_m + A_i(\epsilon_t - \epsilon_m)] = 0$, which in general requires a negative real part of the dielectric function $\text{Re}(\epsilon_t) < 0$ (e.g. for the tip in air with $\epsilon_m \simeq 1$). With $\epsilon(\omega)$ ranging from $(-1.3 + 5.7i)$ to $(-31 + 2.2i)$ for Au and $(4.6 + 17i)$ to $(3.3 + 19i)$ for W in the spectral range of
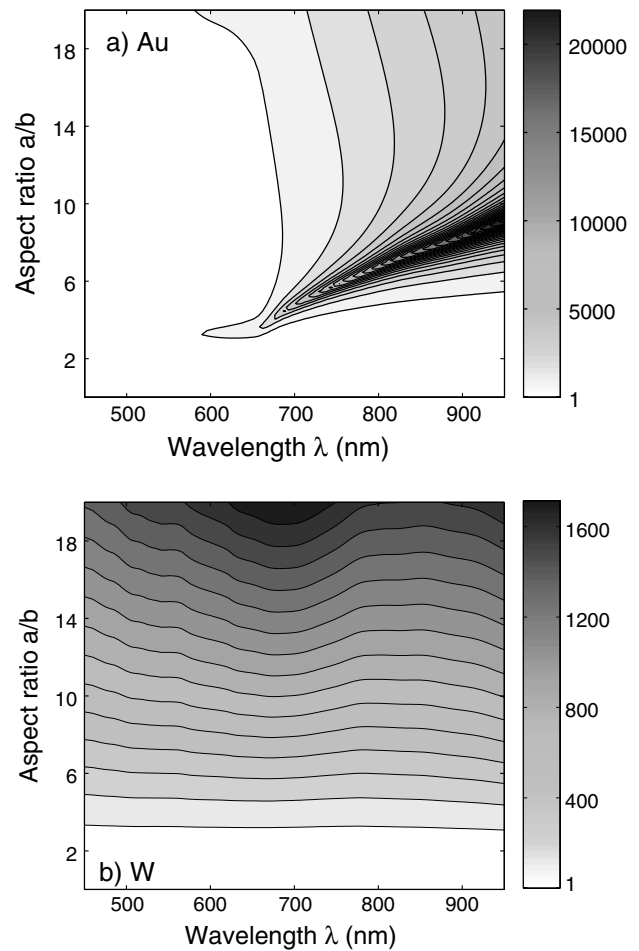
FIGURE 5   Relative polarizability of Au (**a**) and W (**b**) hemispheroids as function of aspect ratio and excitation wavelength calculated using the electrostatic model described in the text. The strongly plasmon-resonant behavior in this wavelength range for Au contrasts a comparatively weak and spectrally flat response for W

450–850 nm [24], it is seen that only Au as a nearly free electron metal would allow for a strong plasmon-resonant polarizability. This is responsible for the fundamentally different optical responses observed for the two metals investigated.

Using this model the dependence of the polarizability along the major axis is plotted in Fig. 5 as a function of both wavelength and aspect ratio a/b for a hemispheroid. In agreement with the experiment, the optical response for Au is dominated by a strong plasmon resonance in this wavelength range, contrasting the spectrally flat and weak response for W. As can be seen, the spectral position of the Au plasmon resonance is very sensitive with respect to the aspect ratio of the hemispheroid. This is in accordance with the experimental observation, where the tip plasmon for Au is found to depend critically on geometric details of the tip apex. Comparing the peak positions of the spectra for the tips investigated with the results of this model, one can attribute aspect ratios in the range from 2 to 6 to describe the actual tip geometries. This is approximately consistent with the tip structures observed in scanning electron microscopy.

The appearance of multiple resonances for inhomogeneous tips is readily explained considering different confined

regions at the apex, which correspond to different resonant conditions. Likewise, observing the scattering response polarized parallel or perpendicular to the tip axis, in the hemispheroidal model this would correspond to the excitation either parallel or perpendicular to its major or minor axis, respectively, which results in two distinct resonance positions. The spectral modulation for the case of the W tip with the long aspect ratio is reproduced by this model as well, where the polarizability becomes increasingly wavelength dependent with increasing aspect ratio.

We emphasized that in the electrostatic model the tip polarization would depend only on the aspect ratio and be independent of the absolute tip dimensions and thus the value of the apex radius. This is supported by our experimental findings, which indicate that the optical response of the tip is more sensitive to the shape of the tip rather than the apex radius alone.

The model discussed here thus provides a qualitative understanding of the tip scattering response. Concerning quantitative values, the electrostatic approximation should be viewed as an upper limit for local-field enhancement and tip polarization. Because of the finite size of the tip, both polarizability and degree of local-field enhancement would be diminished [26]. They rapidly decrease when the structure size increases beyond $\sim\lambda/10$ [27] with the induced polarization distribution of different parts of the emitter becoming increasingly out of phase and thus destructively interfering. However, the model can readily be generalized to the exact Mie theory, to include retardation, radiation damping, and small-size effects [21, 28] and for other model geometries.[1] This, however, would not alter the general conclusion drawn above.

The polarizability α would translate into values for the local-field enhancement L at the tip apex defined by $E_{loc}(\omega) = L E(\omega)$ with $L \simeq 3\alpha_i/4\pi b^2 a$ [23, 25]. Its spectral characteristics would thus follow that of the polarizability within this approximation. Values for the local-field enhancement, however, cannot be derived in this experiment without an absolute reference. They have been determined previously for both Au and W tips for certain wavelengths by means of second-harmonic generation [15] or tip-enhanced Raman scattering [9], with corresponding values found to range from 8 to 25 for Au tips and 3 to 6 for both W and Pt(Ir) at $\lambda \sim 800$ nm.

5   Conclusion

The results presented here with the distinct behavior observed for Au tips characterized by a strong plasmonic response contrasting the dielectric-like scattering for W can be generalized for other tip materials comparing the dielectric functions for different metals. This implies that for other nearly free electron metals such as Al or Ag plasmonic behavior with large polarizability and local-field enhancement is expected. In contrast, similar to the case of W, for example,

Pt(Ir) alloy tips which are frequently applied in AFM-related studies have poor optical properties due to the strong absorption in the UV-vis spectral range.

In our study the optical coupling of the tip to the quartz prism substrate could be neglected. This optical near-field interaction of the tip in close proximity to the substrate is the essence of scattering-type scanning near-field optical microscopy and spectroscopy (s-SNOM). In the case of a weak coupling, as is the case for optically dissimilar tip and sample materials, the tip-scattered light in general would then be a spectral superposition of the optical response of the tip and the spectral properties of the polarization driven by the localized near field in the substrate. This has to be considered in nanospectroscopy especially in the UV-vis spectral region whenever the spectral signature of the sample becomes comparable to that of the tip. In addition, for metallic substrates, strong tip–sample coupling results in characteristic changes of the spectral response of the tip-scattered light [29]. This is accompanied by a large field built up in the tip–sample gap region for parallel polarization [14]. Moreover, the presence of the tip breaks the requirement for parallel momentum conservation in the sample plane and thus allows for additional surface modes to be induced [30].

Achieving good performance in s-SNOM is reportedly sensitive to structural details of the tip, which are found to be hard to reproduce, resulting in a low yield of suitable tips for these experiments. This could be explained by the large variability of the spectral response observed in our study, which would translate into a large variation of the efficacy of near-field enhancement, in particular for excitation at a fixed laser frequency. The results presented here thus provide the necessary criteria for the selection of suitable tips. One way for obtaining tips with well-defined plasmonic response, although at the expense of a large field enhancement, has been demonstrated by attaching gold metal clusters to the apex of glass-fiber-based tips [32, 33]. It can be envisioned, however, that ongoing improvements in the preparation techniques will allow for an optimization of the geometric parameters of the tips by means of ion-beam milling or lithographic techniques and thus tailoring of the optical response for the performance needed in respective applications.

REFERENCES

1 W.L. Stutzman, G.A. Thiele, *Antenna Theory and Design* (Wiley, New York, 1998)
2 W. Denk, D.W. Pohl, J. Vac. Sci. Technol. B **9**, 510 (1991)
3 Y. Wang et al., Appl. Phys. Lett. **85**, 2607 (2004)
4 V.A. Markel, T.F. George (Eds.) *Optics of Nanostructured Materials* (Wiley, New York, 2001)
5 S. Kawata (Ed.) *Topics in Applied Physics* (Springer, Heidelberg, 2001)
6 J.P. Fillard, *Near Field Optics and Nanoscopy* (World Scientific, Singapore, 1997)
7 N. Nilius, N. Ernst, H.-J. Freund, Phys. Rev. Lett. **84**, 3994 (2000); N. Nilius, N. Ernst, H.-J. Freund, Phys. Rev. B **65**, 115421 (2002)
8 R. Hillenbrand, F. Keilmann, Phys. Rev. Lett. **85**, 3029 (2000)
9 A. Hartschuh, E.J. Sánchez, X.S. Xie, L. Novotny, Phys. Rev. Lett. **90**, 095503 (2003)

---

[1]Concerning the notion of optical antennas for the tips, a dipole antenna behavior ($l = n\lambda + \lambda/2$ with $n = 0, 1, \ldots$) is expected only for very slender highly conductive rods with diameter small compared to their length l [1]. Retardation and the considerable loss in the visible spectral region diminish the radiation efficiency.

10 T. Ichimura, N. Hayazawa, M. Hashimoto, Y. Inouye, S. Kawata, Phys. Rev. Lett. **92**, 220801 (2004)
11 N. Ocelic, R. Hillenbrand, Nat. Mater. **3**, 606 (2004)
12 L. Novotny, R.X. Bian, X.S. Xie, Phys. Rev. Lett. **79**, 645 (1997)
13 J.T. Krug II, E.J. Sànchez, X.S. Xie, J. Chem. Phys. **116**, 10895 (2002)
14 J.A. Porto, P. Johansson, S.P. Apell, T. López-Ríos, Phys. Rev. B **67**, 085409 (2003)
15 C.C. Neacsu, G.A. Reider, M.B. Raschke, in preparation
16 L. Aigouy et al., Appl. Phys. Lett. **76**, 397 (2000)
17 M. Moskovits, Rev. Mod. Phys. **57**, 783 (1985)
18 G.C. Schatz, R.P.V. Duyne, in: *Handbook of Vibrational Spectroscopy*, J.M. Chalmers P.R. Griffiths (Eds.) (Wiley, Chichester, 2002)
19 F. de Fornel (Ed.), *Evanescent Waves* (Springer, Berlin, 2001)
20 J.P. Ibe et al., J. Vac. Sci. Technol. A **8**, 3570 (1990)
21 J. Gersten, A. Nitzan, J. Chem. Phys. **73**, 3023 (1980)
22 C.K. Chen, T.F. Heinz, D. Ricard, Y.R. Shen, Phys. Rev. B **27**, 1965 (1983)
23 C.F. Bohren, D.R. Huffman, *Absorption and Scattering of Light by Small Particles* (Wiley, New York, 1998)
24 E.D. Palik (Ed.), *Handbook of Optical Constants of Solids* (Academic, San Diego, 1985)
25 V.M. Shalaev, in: *Springer Tracts in Modern Physics* (Springer, Berlin, 2000)
26 Y.C. Martin, H.F. Hamann, H.K. Wickramasinghe, J. Appl. Phys. **89**, 5774 (2001)
27 N. Calander, M. Willander, J. Appl. Phys. **92**, 4878 (2002)
28 A. Wokaun, J.P. Gordon, P.F. Liao, Phys. Rev. Lett. **48**, 957 (1982)
29 P. Johansson, Phys. Rev. B **58**, 10823 (1998)
30 P.K. Aravind, R.W. Rendell, H. Metiu, Chem. Phys. Lett. **85**, 396 (1982)
31 N. Nilius, N. Ernst, H.-J. Freund, Phys. Rev. B **65**, 115421 (2002)
32 O. Sqalli, U.P. Hoffmann, F. Marquis-Weible, J. Appl. Phys. **92**, 1078 (2002)
33 T. Kalkbrenner, M. Ramstein, J. Mlynek, V. Sandoghdar, J. Microsc. **2002**, 72 (2001)